microbial biotechnology

Open Access

How water-soluble saccharides drive the metabolism of lactic acid bacteria during fermentation of brewers' spent grain

Marta Acin-Albiac,[1] Pasquale Filannino,[2] Rossana Coda,[3] Carlo Giuseppe Rizzello,[4] Marco Gobbetti[1] and Raffaella Di Cagno[1]

[1]*Faculty of Science and Technology, Free University of Bolzano, Bolzano, 39100, Italy.*

[2]*Department of Soil, Plant and Food Science, University of Bari Aldo Moro, Bari, 70126, Italy.*

[3]*Department of Food and Nutrition, Helsinki Institute of Sustainability Science, University of Helsinki, Helsinki, 00100, Finland.*

[4]*Department of Environmental Biology, Sapienza University of Rome, Rome, 00185, Italy.*

Summary

We proposed a novel phenomic approach to track the effect of short-term exposures of *Lactiplantibacillus plantarum* and *Leuconostoc pseudomesenteroides* to environmental pressure induced by brewers' spent grain (BSG)-derived saccharides. Water-soluble BSG-based medium (WS-BSG) was chosen as model system. The environmental pressure exerted by WS-BSG shifted the phenotypes of bacteria in species- and strains-dependent way. The metabolic drift was growth phase-dependent and likely underlay the diauxic profile of organic acids production by bacteria in response to the low availability of energy sources. Among pentosans, metabolism of arabinose was preferred by *L. plantarum* and xylose by *Leuc. pseudomesenteroides* as confirmed by the overexpression of related genes. Bayesian variance analysis showed that phenotype switching towards galactose metabolism suffered the greatest fluctuation in *L. plantarum*. All lactic acid bacteria strains utilized more intensively sucrose and its plant-derived isomers. Sucrose-6-phosphate activity in *Leuc. pseudomesenteroides* likely mediated the increased consumption of raffinose. The increased levels of some phenolic compounds suggested the involvement of 6-phospho-β-glucosidases in β-glucosides degradation. Expression of genes encoding β-glucoside/cellobiose-specific EII complexes and phenotyping highlighted an increased metabolism for cellobiose. Our reconstructed metabolic network will improve the understanding of how lactic acid bacteria may transform BSG into suitable food ingredients.

Received 9 February, 2021; revised 20 April, 2021; accepted 12 May, 2021.

For correspondence. E-mail raffaella.dicagno@unibz.it; Tel. +39 0471 017216; .

Microbial Biotechnology (2022) **15**(3), 915–930
doi:10.1111/1751-7915.13846

Funding information

This transnational project is part of the ERA-Net SUSFOOD2 with funding provided by national/regional sources [FORMAS, Sweden; Ministry of Agriculture and Forestry of Finland; MIUR, Ministero Italiano dell'Università e della Ricerca] and co-funding by the European Union's Horizon 2020 research and innovation programme.

Introduction

The smart management of huge amounts of agro-food by-products has become an area of major environmental and economic importance worldwide. Brewers' spent grain (BSG), the most abundant by-product generated in the beer-brewing process (Mussatto, 2014), represents an example of valuable raw material and source of health promoting compounds (Lynch *et al.*, 2016). BSG is a lignocellulosic substrate, the major constituents of which are fibre (hemicellulose and cellulose) (30–50%), proteins (15–25%) and lignin (12–28%) (Mussatto, 2014). Hemicellulose, primarily consisting of non-cellulose polysaccharide arabinoxylan (AX), is the main BSG constituent, whose backbone is composed of β-(1,4)-linked xylose residues, which can be substituted with arabinose residues while ferulic acid can be esterified on the arabinose residue (Mendis and Simsek, 2014). Besides fibre and proteins, BSG is also a source of free amino acids, minerals, and a variety of phenolic compounds (e.g. phenolic acids), which make BSG an attractive raw material for application in the human diet (Ktenioudaki *et al.*, 2012). Direct extractions of target molecules (e.g. dietary fibres and polyphenols) through traditional technologies such as enzyme-catalysed hydrolysis and solvent extraction have been applied for lignocellulosic substrate recycling (Shalini and Gupta, 2010). However, bioprocessing, using microbes is a versatile, sustainable and promising route for the growing slate of by-products. Recently, BSG fermentation with *Lactiplantibacillus plantarum* under liquid or semi-liquid

conditions was shown to promote the release of bioactive compounds (Verni *et al*., 2020). A BSG/water mixture was also proposed as suitable substrate for dextran biosynthesis by *Leuconostoc pseudomesenteroides* and *Weissella confusa* strains (Koirala *et al*., 2021). Conversion of lignocellulosic substrate to value-added chemicals comprises two main steps: (i) the pre-treatment and the enzymatic hydrolysis to obtain fermentable sugars; and (ii) the fermentation process to produce/release valuable compounds. To date, most of the investigations has been focused on the first step, aiming to optimize the breakdown of the recalcitrant and complex structure of lignocellulosic substrate. Nevertheless, lactic acid bacteria may be severely distressed during the fermentation step by lignocellulose-derived inhibitors (e.g. phenolics, organic acids), in addition to other challenging conditions, such as the limitation of energy sources. Monosaccharides or oligosaccharides from plant biomass can trigger signalling pathways resulting in the activation of transcriptional regulators. On the other hand, efficient utilization of sugars derived from BSG (sucrose, palatinose, trehalose, cellobiose, raffinose and pentosans) would greatly enhance the BSG exploitation. Therefore, a better understanding of bacterial response and adaptation to BSG is critical to select proper starters for efficient BSG bioprocessing. Adaptation to plant lignocellulosic ecosystems markedly vary within species of lactic acid bacteria (Tarraran and Mazzoli, 2018). This is because of the diversity of the plant environments, which reflects on the microbial capacity to share metabolic energy between biosynthesis (e.g. use of alternative substrates) and maintenance (e.g. global stress responses) (Redon *et al*., 2005). Metabolic efficiency is among the primary driving forces of bacterial adaptability, which in turn may result in good fitness (Teusink *et al*., 2006). Among omics technologies, the emerging phenomics has the potential to unravel metabolic traits specific for bacterial niche-adaptation and metabolic and functional diversities at species and strain levels (Filannino *et al*., 2016; Filannino *et al*., 2018a; Acin-Albiac *et al*., 2020). In this study, we proposed a phenomic approach based on the phenotype switching to track the effect of short-term exposures of *L. plantarum* and *Leuc. pseudomesenteroides* to environmental pressure induced by BSG water-soluble saccharides. Capability of both species to grow on BSG-derived substrates was previously reported (Verni *et al*., 2020; Koirala *et al*., 2021). The 'phenotype switching' is a novel concept concerning the assessment of how the bacterial metabolism behaves in growth models (e.g. food-like conditions) differing from standard rich media (e.g. MRS) (Filannino *et al*., 2016, 2018a; Acin-Albiac *et al*., 2020). Phenotype switching was furtherly complemented and validated through differential expression of genes involved in the adopted metabolic strategies.

Results

Kinetics of growth and organic acids production during fermentation of the water-soluble BSG-based medium (WS-BSG)

WS-BSG medium was used as model system to mimic the chemical compositions of the brewers' spent grains. Apart from the species, all strains grew under WS-BSG conditions showing almost the same ($P > 0.05$) increase of cell density (A) (Table 1). *Leuc. pseudomesenteroides* DSM 20193 had the highest maximum growth rate (μ_{max}) in MRS and WS-BSG, 0.62 ± 0.01 and 0.38 ± 0.02 h^{-1} respectively. *L. plantarum* strains had a longer lag phase (λ) compared with *Leuc. pseudomesenteroides* DSM 20193. As expected, when cultivated in the rich MRS medium, all bacteria showed an increase (ca. one and a half more log cycle) of the cell density (CFU ml^{-1}) compared with the cultivation in WS-BSG medium. Consequently, MRS (6.50 ± 0.01 initial pH) was subjected to a strong acidification by all strains, with a ΔpH of 1.95 ± 0.09, 2.45 ± 0.11, 2.59 ± 0.10 and 2.28 ± 0.08 for *Leuc. pseudomesenteroides* DSM 20193, *L. plantarum* WCFS1, PU1 and H46 respectively. The values of μmax and λ calculated based on the data modelling growth were almost consistent with the final cell densities. Due to the low initial pH values (4.62 ± 0.03), the WS-BSG medium was subjected to mild lactic acidification with a ΔpH of 0.35 ± 0.04, 0.53 ± 0.03, 0.46 ± 0.04 and 0.32 ± 0.02 for *Leuc. pseudomesenteroides* DSM 20193, *L. plantarum* WCFS1, PU1 and H46 respectively. Kinetics of organic acids production were determined throughout 24 h of growth in WS-BSG medium (Fig. 1), and the production rate was calculated as the slope of the linear regression for a time range. Lactic acid was always the major fermentation end product. The cultivation of all strains in WS-BSG medium induced a diauxic production of lactic acid (Fig. 1). *Leuc. pseudomesenteroides* showed the first exponential phase from 8 to 13 h with a rate of 0.45 ± 0.07 mM h^{-1} and a final concentration of lactic acid of ca. 2.71 mM. The first exponential phase for *L. plantarum* strains, appeared after 6 h and lasted up to 8 h of fermentation with a rate that ranged from 2.67 ± 0.13 (PU1) up to 2.77 ± 0.16 mM h^{-1} (WCFS1), and a production of ca. 5.40 mM. H46 showed the first increase of lactic acid from 4 to 6 h (0.39 ± 0.02 mM h^{-1}; 0.91 ± 0.02 mM). The second lag phase, suggesting a metabolic switch, lasted from 8 to 16 h for *L. plantarum* PU1, H46 and *Leuc. pseudomesenteroides* DSM 20193, and from 8 to 12 h for WCFS1. Lactic acid production rate during the second exponential phase decreased with respect to the first phase, which was 0.37 ± 0.10 mM h^{-1} for DSM 20193,

Table 1. Parameters of the growth kinetic of *Lactiplantibacillus plantarum* and *Leuconostoc pseudomesenteroides* strains during fermentation of brewers' spent grains (WS-BSG) and MRS media at 30°C for 24 h.

Media[a]	Species/strain	Maximum Growth[b] (Log CFU ml^{-1})	μmax (Log CFU ml^{-1} h^{-1})	λ (h)
WS-BSG	*Lactiplantibacillus plantarum* WCFS1	8.45 ± 0.04^{D}	0.24 ± 0.01^{E}	4.76 ± 0.14^{B}
	L. plantarum PU1	8.43 ± 0.01^{D}	0.21 ± 0.01^{F}	5.17 ± 0.12^{A}
	L. plantarum H46	8.22 ± 0.01^{E}	0.18 ± 0.01^{F}	4.43 ± 0.06^{C}
	Leuconostoc pseudomesenteroides DSM20193	8.48 ± 0.02^{D}	0.38 ± 0.02^{D}	3.63 ± 0.14^{D}
MRS	*L. plantarum* WCFS1	9.82 ± 0.02^{A}	0.58 ± 0.01^{B}	2.21 ± 0.12^{E}
	L. plantarum PU1	9.73 ± 0.03^{B}	0.53 ± 0.01^{C}	$2.38 \pm 0.06^{D,E}$
	L. plantarum H46	9.85 ± 0.01^{A}	0.53 ± 0.03^{C}	$2.33 \pm 0.15^{D,E}$
	Leuc. pseudomesenteroides DSM20193	9.53 ± 0.03^{C}	0.62 ± 0.01^{A}	1.47 ± 0.06^{F}

a. For the manufacture of the media, see Materials and Methods.
b. Growth data were modelled according to the logistic equation available in *grofit* R package (Kahm *et al*., 2010). Parameters for growth: A, maximum absorbance reached by the culture at the stationary phase of growth (log CFU ml^{-1}); μ_{max}, maximum growth rate (log CFU ml^{-1} h^{-1}); λ, length of the lag phase (h). Means within the columns followed by different letters (A to E) are significantly different ($P < 0.05$). Shown are mean values ± standard deviations for the three batches of each type of media, analysed in duplicate.

0.40 ± 0.03 mM h^{-1} for PU1, 0.41 ± 0.01 mM h^{-1} for H46 and 0.74 ± 0.13 mM h^{-1} for WCFS1 with a final concentration of 4.46 ± 0.39, 8.90 ± 0.19, 2.30 ± 0.05 and 8.56 ± 0.32 mM respectively. Synthesis of lactic acid by *L. plantarum* WCFS1 reached a *plateau* after 20 h of fermentation (8.70 ± 0.38 mM). During WS-BSG fermentation, the production of acetic acid by *Leuc. pseudomesenteroides* DSM 20193 displayed a single metabolic phase, which started after 6 h with a rate of 0.23 ± 0.01 mM h^{-1} and increased up to 16 h (1.49 ± 0.23 mM). The production of acetic acid by *L. plantarum* strains was found from 6 to 8 h with a rate of 0.46 ± 0.07, 0.67 ± 0.06, and 0.17 ± 0.00 mM h^{-1} for *L. plantarum* PU1, WCFS1 and H46 respectively. The final concentration (at 8 h) of acetic acid was 1.05 ± 0.10, 2.30 ± 0.07 and 0.87 ± 0.01 mM respectively. Similarly to lactic acid kinetics, *L. plantarum* WCFS1 showed a second lag phase for acetic acid (from 8 to 12 h) and a second exponential phase with a lower production rate (0.11 ± 0.02 mM h^{-1}). When cultivated in MRS medium, the concentration of lactic and acetic acids markedly increased, but the ratio acetic–lactic acids was lower than WS-BSG. Due to the low levels of glucose, fructose and sucrose in WS-BSG medium (Table S1), after 24 h of fermentation these carbohydrates were below the limit of detection of the instrument. Citric and malic acids were not detected throughout the fermentation trials.

Phenotypic profiles adaptation to brewers' spent grain ecosystem

A phenotypic screen for *L. plantarum* PU1, H46 and WCFS1 and *Leuc. pseudomesenteroides* DSM 20193 in WS-BSG medium compared with the MRS was reconstructed by using the Phenotype MicroArray Omni-Log PM technology (Biolog, Hayward, CA, USA) (Figs 2, 3, S2 and S3; Dataset S1 in Supplementary Information) Cells of PU1, H46, WCFS1 and DSM 20193 were collected during the late exponential (LE) growth phase and used to inoculate the PM plates. The range of phenotypes analysed included the transport, uptake and catabolism of 190 carbon sources. For *L. plantarum* strains, the effect of genotypic traits (H46, PU1 and WCFS1), that of culture media (WS-BSG and MRS), the evolution of such effects and metabolism dynamics were determined among phenotypes (Figs 3, S2 and S3 in the Supplementary material). The area under the curve (AUC) of phenotype grouped the assayed conditions in two big clusters (Fig. 2) based on the genus (*Leuconostoc* spp. and *Lactiplantibacillus* spp.). Clustering of *L. plantarum* phenotypes was media dependent and not by strain genotypic traits. All strains showed a higher metabolic performance for a wider range of carbon sources when cultured in WS-BSG medium (average AUC equal to 3218 ± 174 OL·h) compared with MRS (average AUC equal to 2475 ± 227 OL·h). This increase in activity was also reflected on higher metabolic rates and shorter lag phases for many compounds (Dataset S1).

Among hexoses, galactose metabolism-related compounds appeared to play a pivotal role in the metabolism of *L. plantarum* strains when grown in WS-BSG medium. For instance, β-galactosides such as lactose, lactulose and galactose were highly metabolized by *L. plantarum* WCFS1 and PU1 strains. On the contrariwise, *Leuc. pseudomesenteroides* DSM 20193 shifted his metabolism towards raffinose and melibiose. The latter was also used by *L. plantarum* strains. Analysis of variance applied to the phenotypic response of *L. plantarum* strains revealed that compounds related to galactose

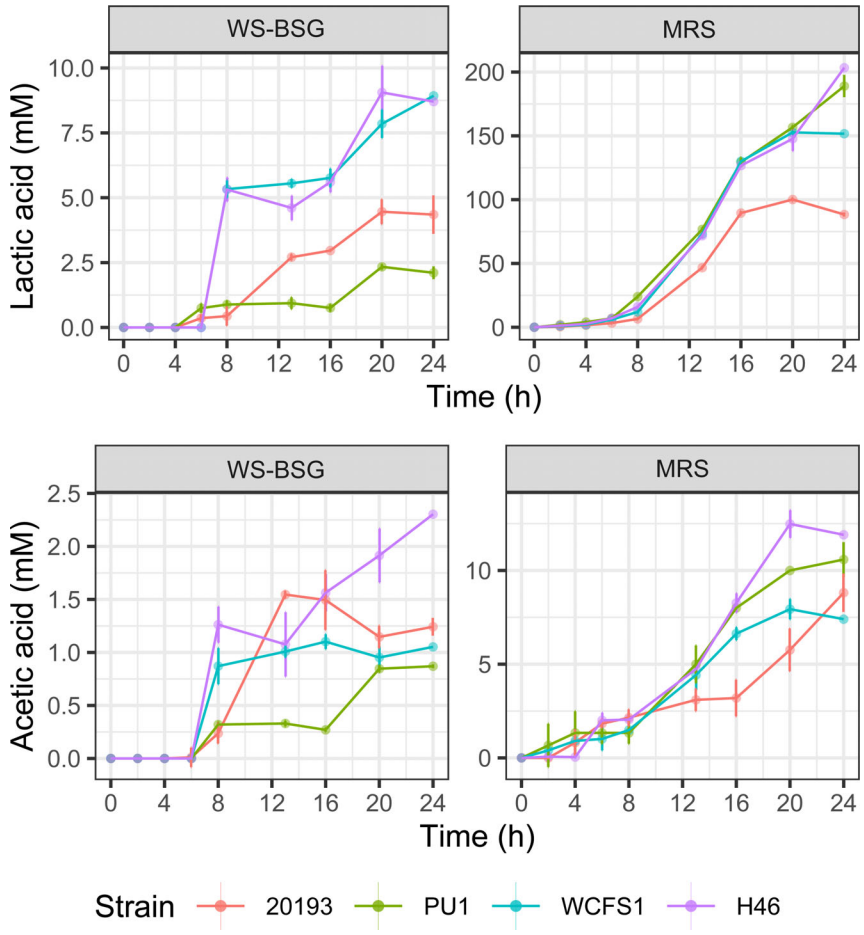

Fig. 1. Organic acids production (mM) of *Leuconostoc pseudomesenteroides* DSM 20193 and *Lactiplantibacillus plantarum* PU1, H46 and WCFS1 during fermentation of brewers' spent grains (WS-BSG) at 30°C for 24 h.

metabolism were the ones that suffered most from the strain's effect and the shifting of the medium (Fig. 3). In particular, PU1 showed the most significant ($P < 0.05$) metabolic switch for D-lactose, lactulose, D-melibiose and D-galactose when moved from MRS to WS-BSG. However, the enhanced metabolic response of PU1 on WS-BSG occurred at different times during the experiment evolution (Fig. 3).

Starch and sucrose metabolism compounds such as sucrose, palatinose, D-cellobiose and salicin were intensively metabolized when *L. plantarum* H46 and PU1 were grown in WS-BSG medium (Fig. 3). *Leuc. pseudomesenteroides* DSM 20193 and *L. plantarum* PU1 under WS-BSG conditions showed a higher metabolism for sucrose and its related isomers and oligosaccharides compared with MRS, especially, *L. plantarum* strains metabolized palatinose, trehalose and melezitose while *Leuc. pseudomesenteroides* consumed palatinose, trehalose and turanose (Fig. 3C). Among *L. plantarum* strains, PU1 and H46 showed the highest ($P < 0.05$) sucrose consumption especially during the exponential phase of the metabolism (Fig. 3B), which corresponded with a higher increase of the metabolic rate for this compound compared with MRS. Sucrose subunits (glucose and fructose) were also strongly metabolized by PU1. Besides, the cultivation of PU1 in WS-BSG medium highly stimulated the palatinose metabolism compared with the other sucrose isomers. *L. plantarum* and *Leuc. pseudomesenteroides* strains differentially metabolized cellobiose and gentiobiose (Fig. 2). 6-Phospho-β-glucosidases (EC. 3.2.1.86) are responsible for the degradation of β-glucosides such as cellobiose and gentiobiose as well as glycosylated phenolic compounds, which are widespread among plant matrixes. Salicin metabolism was also found in all strains (Fig. 3A), where PU1 showed the highest and significant ($P < 0.05$) metabolic use when cultured in WS-BSG (Fig. 3B). The WS-BSG effect takes place during the exponential phase of salicin metabolism kinetics.

Substrates involved in pentose and glucoronate interconversions pathway (e.g. arabinose, xylose, D-galacturonic acid and pectin) were also highly

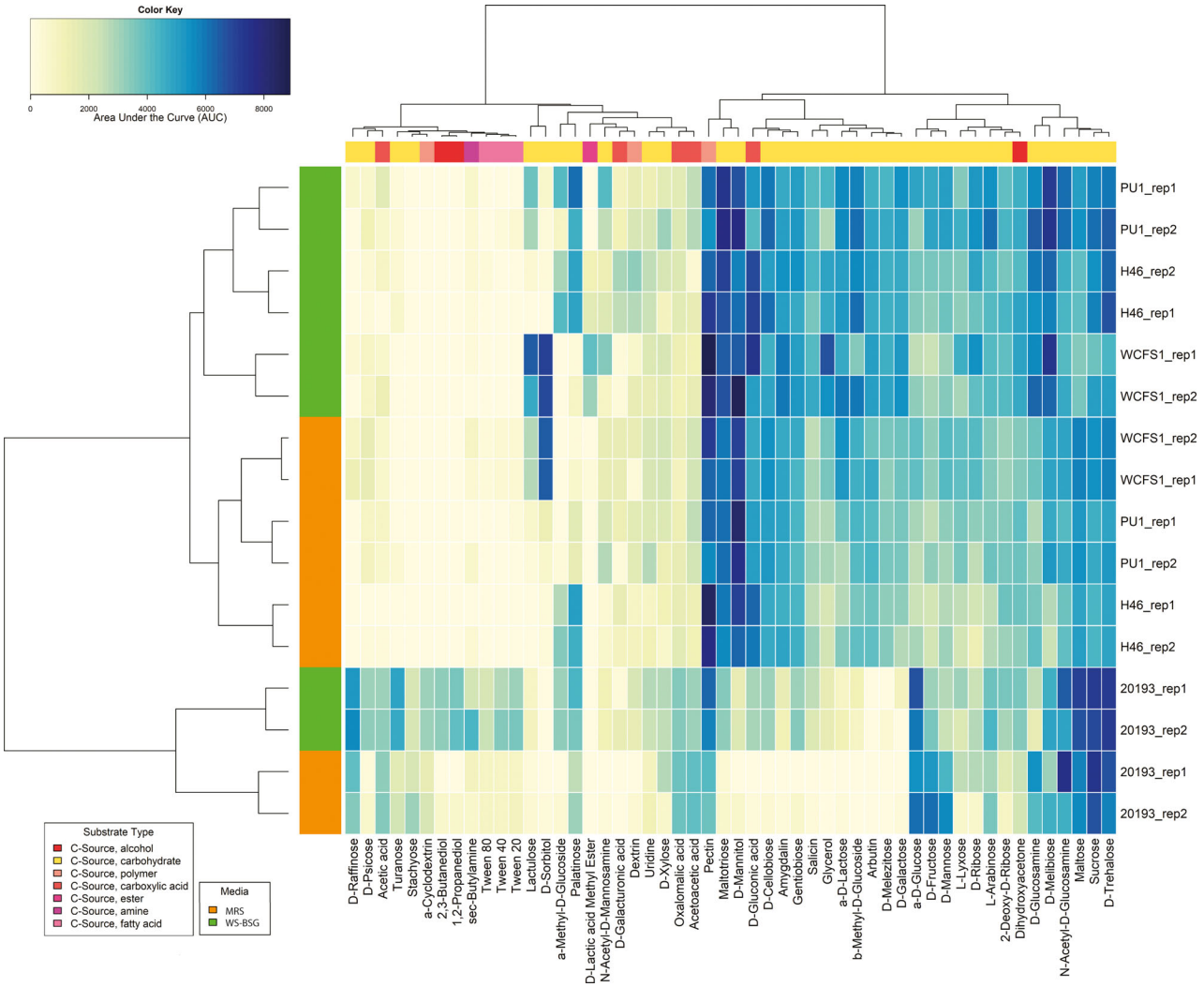

Fig. 2. Comparison of phenotypes of *Leuconostoc pseudomesenteroides* DSM 20193 and *Lactiplantibacillus plantarum* PU1, H46 and WCFS1 previously cultivated on water-soluble BSG-based medium (WS-BSG) until the late exponential (LE) phase of growth (16 h) at 30°C was reached. All strains were also cultivated on MRS broth (MRS) used as control medium under the same conditions (LE phase of 8 h at 30°C). The colour scale shows differences in term of the area under the curve (AUC), with a gradient from yellow to blue indicating the lowest and highest values of the AUC respectively. Each phenotype profile was assayed for growth in the presence of various carbon using Omnilog Phenotype MicroArray, as described in the Materials and Methods. Raw data are reported in the Supplementary Information (Dataset S1).

metabolized in WS-BSG compared with MRS condition. *Leuc. pseudomesenteroides* DSM 20193 was the only strain able to actively metabolize D-xylose. *Leuc. pseudomesenteroides* DSM 20193 and *L. plantarum* WCFS1 metabolized pectin, whereas *L. plantarum* H46 was the only able to actively consume D-galacturonic acid. *L. plantarum* WCFS1 preferred D-gluconic acid rather than glucose compared with the other strains and to MRS. *L. plantarum* strains showed an increased metabolism for L-arabinose under WS-BSG conditions compared with MRS. The metabolic switch towards an arabinose consumption rate was highly significant ($P < 0.05$) for PU1 both in exponential and stationary phases of the metabolism (Fig. 3).

In order to better highlight their metabolic performances of the three strains of *L.* plantarum during WS-BSG fermentation compared with MRS, the proportion of strain and media significant effects computed at different time points of metabolic kinetics was used (Fig. 3C). This analysis was used to determine the strain with the highest metabolic switch from MRS to WS-BSG conditions. *L. plantarum* H46 showed a similar basal metabolism compared with PU1, but the first one was not subjected to an overall significant switching when cultured on WS-BSG. Although WCFS1 seemed to be more performing from a baseline metabolic point of view than PU1 when they were cultured in MRS, PU1 showed a metabolic switch towards the degradation of a widest

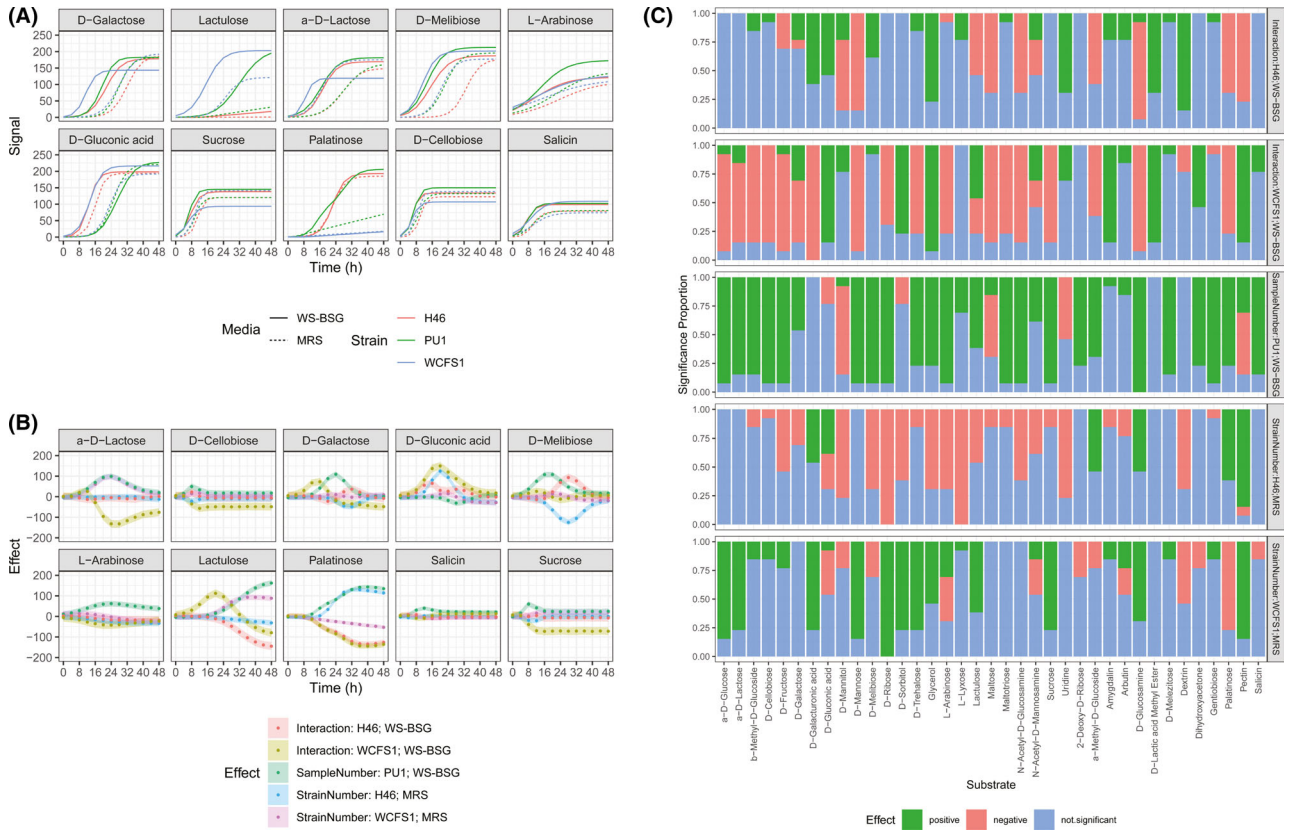

Fig. 3. Effect of *Lactiplantibacillus plantarum* strains (PU1, H46 and WCFS1) and culture media [water-soluble BSG-based medium, WS-BSG and MRS] and their interaction on the metabolism of selected compounds (A) Logistic median metabolic curves of selected profiles for *L. plantarum* strains cultured in WS-BSG (continuous line) and MRS (dashed line). (B) Estimate effects and 95% Bayesian credibility intervals over time computed as the mean values of Markov chains produced by the variance analysis model. MRS – *L. plantarum* PU1 represents the reference condition. (C) Proportion of significant (*P*-value < 0.05) effects respect to the control condition (*Lactiplantibacillus plantarum* PU1-MRS) for all time points evaluated by the variance analysis model. Effects of culture media (WS-BSG and MRS) and strains (*Lactiplantibacillus plantarum* PU1, H46, WCFS1) were determined every 4 h for 48 h of kinetic metabolism. The significance of each factor for every time point can be represented as a proportion respect to all time points evaluated.

range of substrates when cultured on WS-BSG. Having in MRS a metabolic baseline similar to PU1 and not displaying a consistent metabolic switching when cultured in WS-BSG, *L. plantarum* H46 was excluded from further characterizations.

Phenolic profile changes during WS-BSG fermentation

Phenotype switching experiments of bacteria suggested an increased metabolism for glycosylated phenolic compounds (e.g. salicin). We further investigated how WS-BSG phenolic profile changed during 24 h of fermentation. Among ten identified phenolic compounds, *p*-coumaric and especially vanillin and *p*-syringic acid increased during the fermentation (Fig. S4). Generally, the increase occurred linearly during the first 4–8 h except for *L. plantarum* PU1, which started after 16 h and then remained stable throughout the fermentation. The increase in vanillin coincided with the exponential phase of growth of strains.

Comparison of 6-phospho-β-glucosidases encoded in Leuc. pseudomesenteroides *and* L. plantarum *genomes*

Based on bacterial phenotype response and being 6-phospho-β-glucosidases (EC. 3.2.1.86) responsible for the degradation of β-glucosides and glycosylated phenolic compounds, further investigation was carried out. Alignment of protein sequences associated to *pbg* genes of five *L. plantarum* genomes and the reannotated genome of *Leuc. pseudomesenteroides* DSM 20193 gave the phylogenetic tree of Fig. S5. The clustering was annotated according to the association within the operon with cellobiose or generic β-glucosides phosphotransferase transport systems (PTS) of each *pbg* gene. The analysis revealed two main clusters. The most distant cluster included enzymes encoded by *pbg6* genes, which are organized in the operon together with cellobiose PTS. The second cluster includes two main subgroups. The first one groups the enzymes encoded by *pbg* genes (*pbg1*, *pbg4* and *pbg5*), which are associated

to cellobiose PTS genes within the same operon. This subgroup also includes two 6-phospho-β-glucosidase sequences of *Leuc. pseudomesenteroides* DSM 20193 that are closely related to the enzymes codified by *pgb4* and *pbg5* in *L. plantarum* WCFS1. The second subgroup contains protein sequences whose coding *pbg* gene is encounter within the same operon as generic β-glucosides PTS (*pbg2*, *pbg3*, *pbg7*, *pbg8* and *pbg10*). For further gene expression experiments, we selected one *pbg* gene per cluster and subclusters: *pbg6*, *pbg4* and *pbg8* for *L. plantarum* strains. The selected phospho-β-glucosidase of *Leuc. pseudomesenteroides* DSM 20193 was closely related to the amino acid sequence encoded by *pbg4* in *L. plantarum* WCFS1.

Gene expression coding for galactose, sucrose and starch and glucuronate interconversions pathways under brewers' spent grain conditions

Phenotype switch, showing evident fluctuations on specific compounds (β-galactosides, β-glucosides, arabinose, galactose and sucrose), was further deepened. Quantification of the expression of 10 genes involved in galactose metabolism (galactokinases and beta-galactosidases), sucrose and its isomers metabolism (sucrose-6-phosphate hydrolases) and pentose and glucoronate interconversions pathway (L-arabinose and xylose isomerase) was aimed to determine whether particular pathways are over-expressed in response to the WS-BSG substrate (Table S2). Phospho-β-glucosidase activities were also targeted for putative enzymes involved in the degradation of cellobiose (*pbg4* and *pbg6* related genes) and other β-glucosides, such as gentiobiose and glycosylated forms of polyphenolic compounds (*pbg8* gene). For relative quantification, the value of ΔC_T for each sample was determined by calculating the difference between the value of C_T of target genes and the value of C_T of the 16S rRNA housekeeping gene. Then, the value of $\Delta\Delta C_T$ for each sample was determined by subtracting the value of ΔC_T of the calibrator (reference sample) from the ΔC_T value for the sample. The calibrator used for each gene was the strain cultured in MRS. In the case of *L. plantarum strains*, the calibrator was PU1 cultured in MRS for each gene. The normalized level of target gene expression was calculated by using the formula: $2^{>}\Delta C_T$. A gene was considered overexpressed when its RE level was higher than 2 (Desroche *et al*., 2005).

Leuc. pseudomesenteroides DSM 20193 did not show a significant fold change on *xylA* (1.23 ± 1.12) and *INV* genes (3.87 ± 2.14), while *pbg-like* showed an overexpression of 7.83 ± 1.73 fold change after 8 h of incubation in WS-BSG compared to MRS. After 16 h of growth in WS-BSG medium *Leuc. pseudomesenteroides* DSM 20193 showed an overexpression of *INV* (44.7 ± 12.4), *xylA* (65.4 ± 17.4) and *pbg4*-like (13.4 ± 6.0) encoding for sucrose-6-phosphate hydrolase, xylose isomerase and 6-phospho-beta-glucosidase respectively (Fig. 4A).

Overexpression of *LacM* (50.4 ± 9.8) and *galK* (117.1 ± 45.9) genes was found in *L. plantarum* PU1 after 8 h of growth in WS-BSG (Fig. 4B). After 16 h, the metabolism of PU1 switched from β-galactosides and galactose towards arabinose as showed by the high expression of *araA* gene (58.6 ± 20.6). *ScrB* gene coding for sucrose-6-P-hydrolase was also expressed in PU1 after 8 h (14.7 ± 3.9). WCFS1 preferred arabinose during the first growth phase in WS-BSG showing similar fold (54.0 ± 11.5) increase than PU1. On the contrary, the fold change of *LacM* (less than 9) and *galK* (less than 8) was moderate at both time points. *L. plantarum* strains cultured on WS-BSG model medium overexpressed *pbg4* and *pbg6* genes, which are related to cellobiose degradation. The overexpression of *pbg4* was similar (ca. 10) for both strains while *pbg6* was highly overexpressed by PU1 after 8 h (60.3 ± 31.9) of growth. No overexpression was found for *pbg8*.

Correlation among *L. plantarum* WCFS1 and PU1 and growth media (WS-BSG, MRS) based on the normalized data of their mean effects on phenotype switching of selected compounds (D-lactose, lactulose, D-melibiose and D-galactose, palatinose, sucrose, cellobiose and salicin) and gene expression of related genes was calculated (Fig. 4C). Strains cultured on WS-BSG medium are highly correlated with each other and were inversely associated when cultured in MRS.

Discussion

In this study, we generated phenome microarray profiles of *L. plantarum* and *Leuc. pseudomesenteroides* during growth in a water-soluble BSG-based medium (WS-BSG). *L. plantarum* and *Leuc. pseudomesenteroides* were used as model heterofermentative organisms due to their occurrence in plant niches and their role in bioprocessing of lignocellulosic substrates (Verni *et al*., 2020; Koirala *et al*., 2021). The species *L. plantarum* represents the paradigm of nomadic lifestyle within the heterofermentative clade of lactobacilli (Siezen and van Hylckama Vlieg, 2011; Inglin *et al*., 2018). *L. plantarum* is one of the best examples of species with dynamic and flexible behaviour (Duar *et al*., 2017; Filannino *et al*., 2018a). The plant-origin subspecies *Leuc. pseudomesenteroides* DSM 20193 is among those with the largest genome size (1.93 Mb) among 17 subspecies of *Leuconostoc* genus suggesting its ecological fitness in plant-based ecosystems (Özcan *et al*., 2019). The capability to produce dextrans in the presence of sucrose by this

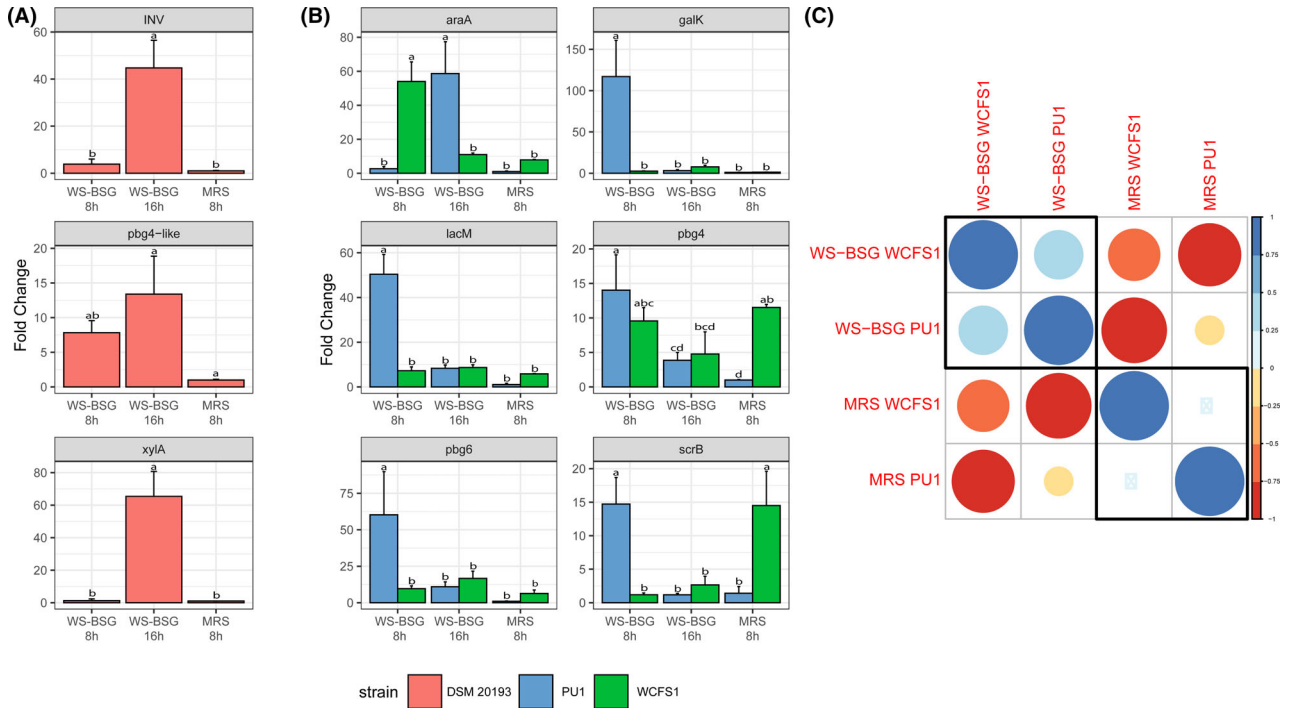

Fig. 4. Relative expression of selected genes *Leuconostoc pseudomesenteroides* DSM 20193 (Panel A) and *Lactiplantibacillus plantarum* PU1 and WCFS1 (Panel B) cultivated on water-soluble BSG-based medium (WS-BSG) until the first (after ca. 8 h) and late (after ca. 16 h) exponential (LE) phase of growth at 30°C were reached. *INV* (sucrose-6-phosphate hydrolase), *xylA* (xylose isomerase) and pbg-like (6-phospho-beta-glucosidase) genes were selected for *Leuc. pseudomesenteroides*, while for *L. plantarum*, *araA* (L-arabinose isomerase), *galK* (galactokinase), *lacM* (beta-galactosidase), *scrB* (sucrose-6-phosphate hydrolase), *pbg4*, *pbg6* and *pbg8* (6-phospho-beta-glucosidases) genes were selected. The calibrator conditions used were the same bacterial cultures grown in MRS until the LE phase of growth (after ca. 8 h) at 30°C was reached. Pearson correlation (Panel C) between *L. plantarum* strain and growth media based on normalized phenotypic mean effects calculated by the variance analysis of selected compounds (D-lactose, lactulose, D-melibiose, D-galactose, palatinose, sucrose, cellobiose and salicin) and gene expression data. Data are the means of three independent experiment analysed in triplicate ± standard deviations.

bacterium (Olvera *et al.*, 2007; Côté and Skory, 2012) was also considered a useful metabolic trait to exploit the BSG. To our knowledge, this study is the first to present whole-phenome data generated from *L. plantarum* and *Leuc. pseudomesenteroides* during fermentation of BSG-derived water-soluble substrate. Our approach combined phenotype switching from MRS to WS-BSG model media with gene expression and a panel of metabolome analyses to get insights into the metabolic strategies adopted by the lactic acid bacteria starters. As expected, WS-BSG represents an example of stressful environment for microbial growth due to a limitation of energy sources, which leaded *L. plantarum* and *Leuc. pseudomesenteroides* to a diauxic profile of organic acids production. The metabolic drift for sugars consumption likely underlay the lower lactic acid production rate during the second exponential phase, as consequence of the different efficiency of substrates conversion and product yields (Guyot and Morlon-Guyot, 2001). We have proposed a WS-BSG adaptive regulation model for *L. plantarum* and *Leuc. pseudomesenteroides*, which is shown in Fig. 5. Phenotype profiling allowed stratifying the metabolic profiles of *L. plantarum* strains according to the culture media (Fig. 2). This finding agrees with metabolic flexibility of *L. plantarum* due to its nomadic lifestyle (Martino *et al.*, 2016; Inglin *et al.*, 2018). Indeed, strains isolated from different habitats may adopt similar metabolic strategies under the same environmental condition (Filannino *et al.*, 2014; Esteban-Torres *et al.*, 2017). The environmental pressure exerted by WS-BSG on *Leuc. pseudomesenteroides* DSM 20193 also markedly shifted its phenotype. All bacteria strains showed a higher metabolic performance for a wider range of carbon sources compared to MRS, which reflects the heterologous variety of complex carbohydrates present in BSG (Robertson *et al.*, 2010; Lynch *et al.*, 2016).

Arabinoxylans are the most abundant pentosans in BSG (Robertson *et al.*, 2010). The higher ratio of acetic/lactic acid found for all bacteria under WS-BSG conditions compared to MRS was related to the pentosans metabolism. Xylose and arabinose catabolic cascade converges in 5P-xylulose within pentose and glucuronate interconversions before shunting to pentose and phosphate pathway, leading to the formation of acetic and ATP (Gobbetti *et al.*, 2000; Gänzle and Follador, 2012).

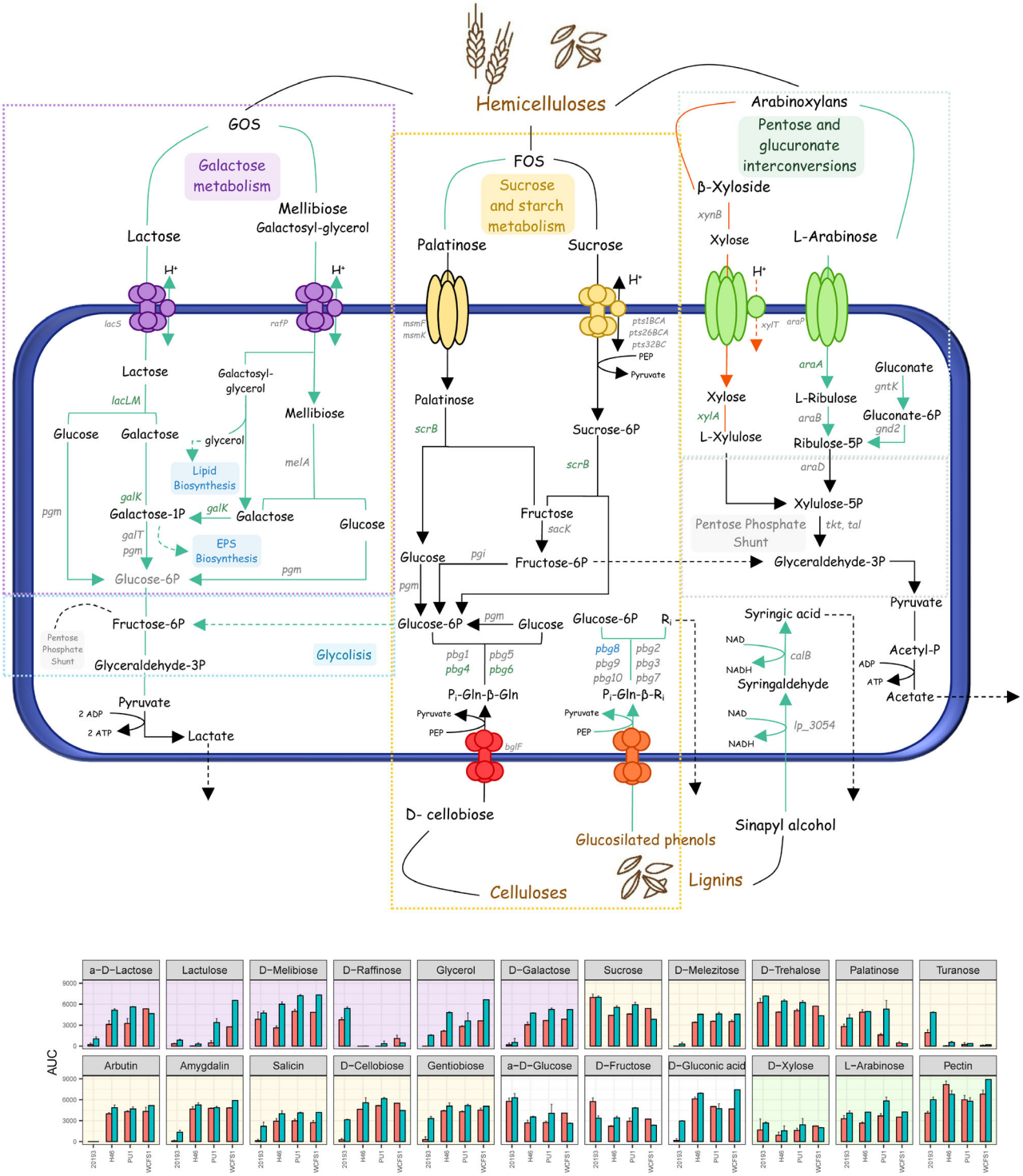

Fig. 5. Schematic representation of the presumptive metabolic pathways in *Leuconostoc pseudomesenterides* DSM 20193 and *Lactiplantibacillus plantarum PU1*, *H46 and WCFS1*, during fermentation of water-soluble BSG-based medium (WS-BSG) at 30°C for 24 h. The schema contains genes relevant for each pathway (grey), over- (green) and non-overexpressed (blue) genes. Phenotypes of strains for selected substrates during the growth on MRS (red bars) and WS-BSG (green bars) are represented in bar plots, where the background is coloured according to the main metabolic pathway as follows: galactose metabolism (purple), starch and sucrose metabolism (yellow), glycolysis / pentose phosphate pathways (white) and pentose and glucuronate interconversions (green). Pathways coloured in orange were present only in *Leuc. pseudomesenteroides* DSM 20193, while pathways coloured in turquoise were only present in *L. plantarum* strains during WS-BSG fermentation. Pathways coloured in black were present in both genera.

Although *L. plantarum* does not possess α-L-arabinofuranosidase activity, release of arabinose by BSG autochthonous microbiota (total cell number of mesophilic bacteria of ca. 5.20 ± 0.14 Log CFU g^{-1}, data not shown) or endogenous enzyme activities during the storage could be not excluded (Lynch *et al.*, 2016). Arabinose may also be forming part of arabinogalactans, which are included in low proportion among BSG hemicelluloses (Robertson *et al.*, 2010; Lao *et al.*, 2020). Arabinose was metabolized more efficiently by all *L. plantarum* strains under WS-BSG conditions, and such metabolic drift was confirmed by gene expression. *L. plantarum* harbours a complete set of genes for arabinose metabolism organized in *araBAD* operon (Mota *et al.*, 1999). The overexpression for *araA* gene under WS-BSG conditions was strain and growth phase-dependent. On the other hand, *Leuc. pseudomesenteroides* DSM 20193 increased the consumption of xylose under WS-BSG conditions, which agrees with the marked increase of *xylA* expression. Some species within *Leuconostoc* spp. possess the capability to ferment xylo-oligosaccharides as confirmed by the presence of *xynB* gene encoding for a 1,4-β-xylosidase in DSM 20193 (Mazzoli *et al.*, 2014). Surprisingly, in-depth Bayesian variance analysis showed that phenotype switching towards galactose metabolism suffered the greatest fluctuation in *L. plantarum* strains under WS-BSG conditions (Fig. 3). Metabolic drift for galactose-related compounds and arabinose was highly significant for *L. plantarum* PU1, which is consistent of PU1 from cheese environment, although all strains could metabolize lactose. In agreement, we found a marked overexpression for *lacM* and *galK* for PU1 during the first metabolic phase (8 h) in WS-BSG medium, while moderate or low fold expression changes were found for WCFS1 at both phases of growth. *LacS* permease is responsible for the intracellular transport of β-galactosides (βGOS) (Thongaram *et al.*, 2017). Once in the cytoplasm, a β-galactosidase encoded by *lacLM* genes breakdown βGOS to galactose and glucose, and the latter is consumed preferentially (Gänzle and Follador, 2012). These findings suggest that PU1 metabolizes large βGOS from WS-BSG through β-galactosidase activity of *lacLM*. Due to the low nutrient availability in WS-BSG, *lacS* may be switched to proton-mediated symport of βGOS (Gänzle, 2012; Zhao and Gänzle, 2018). This would allow the activation of galactose by *galK*, retrieving additional ATP through EMP pathway (Watson *et al.*, 2013).

The presence of sucrose in WS-BSG may derive from residual endosperm starch (Robertson *et al.*, 2010; Lynch *et al.*, 2016). Phenotyping microarray revealed that all lactic acid bacteria strains utilized more intensively sucrose and its plant-derived isomers (e.g. palatinose and D-trehalose) during WS-BSG fermentation. Although *L. plantarum* strains used in this study were isolated from contrasting habitats (e.g. cheese, hemp, and human saliva) they retained the capability to metabolize such substrates as a genetic reminiscence of its original plant-associated lifestyle (Martino *et al.*, 2016). Diverse disaccharide-(phosphate)-glycosylases are found in nomadic lactobacilli species (Gänzle and Follador, 2012). Such enzymes and their respective PTS-complexes are encoded by a block of seven genes comprising the sucrose isomer metabolism *sim* operon in *Lactiplantibacillus casei* (Thompson *et al.*, 2008). *L. plantarum* WCFS1 genome harbours four paralogous sequences with α-glucosidase activity (*malL*, lp_0189, lp_0193 and lp_3220). Two of these genes are allocated in the same cluster of sucrose-6-phosphate hydrolase gene (*scrB*). Recently, a novel oligo-α-1,6-glucosidase encoded by *malL* gene was characterized, displaying a specific activity towards palatinose (Delgado *et al.*, 2017). *L. plantarum* PU1 showed a great metabolic activity switch towards palatinose when cultured on WS-BSG (Fig. 3). In fact, *scrB* was overexpressed in PU1 during WS-BSG growth while WCFS1 did not show any significant increase of fold change in agreement with his phenotype switching. These findings suggest that sucrose and related isomers metabolism may be subjected to a common regulation, which may be strain dependent. We observed a significant fold change of sucrose-6-phosphate hydrolase gene also in *Leuc. pseudomesenteroides* DSM 20193 under WS-BSG conditions. Furthermore, sucrose-6-phosphate activity may also degrade the anti-nutritional factor raffinose, which is reported to be present in BSG (Robertson *et al.*, 2010). Consequently, phenotyping revealed an increased consumption of raffinose by DSM 20193 during WS-BSG fermentation.

Celluloses are the main constituent of BSG husk. Partial hydrolysis of cellulose by endogenous β-glucosidases may occur during BSG storage, yielding to soluble oligosaccharides (Lynch *et al.*, 2016). We further investigated the phylogenetic relationship among *pbg* protein sequences encoding for phospho-β-glucosidase activity harboured by *L. plantarum* and the corresponding homologs present in *Leuc. pseudomesenteroides* DSM 20193. Protein sequences diverged according to the specificity of the PTS complex, which they were associated. Nine of *pbg* genes harboured by *L. plantarum* and phospho-β-glucosidases belonging to *Leuc. pseudomesenteroides* DSM 20193 are allocated adjacent to genes encoding β-glucoside/cellobiose-specific Enzyme II (EII) complexes. Gene expression and phenotyping highlighted an increased metabolism for cellobiose during growth in WS-BSG. Thus, we can state that cellobiose metabolism likely plays a pivotal role

during WS-BSG fermentation in response to its compositional properties (Mussatto, 2014; Lynch *et al*., 2016).

Although all *L. plantarum* strains followed the same metabolic strategies to counteract the limitation of energy sources during WS-BSG fermentation, we hypothesize that the mode of action to pursue such strategies is strain dependent. The growth phase-dependent metabolic drift towards galactose-related compounds, arabinose, sucrose and cellobiose was highlighted, especially for *L. plantarum* PU1.

Most of the phenolic compounds found in BSG are related to lignin macromolecules, which are mainly constituted of syringyl and guaiacyl alcohols (Rencoret *et al*., 2015). The analysis of phenolic compounds revealed that syringic acid was released during WS-BSG fermentation. *L. plantarum* possess a benzyl alcohol dehydrogenase (lp_3054), which may catalyse the oxidation of syringic alcohol (Rodríguez *et al*., 2009). Further oxidation of syringaldehyde to syringic acid is catalysed by specific aldehyde dehydrogenases. Coniferyl aldehyde dehydrogenase is encoded by *calB* gene in *L. plantarum* and may catalyse this reaction due to the high substrate homology between coniferyl and syringaldehyde (Kamimura *et al*., 2017). We speculate that lignin alcohol intermediates degradation through this two-step oxidation may be a source of energy and reducing power derived from growth in WS-BSG conditions (Rodríguez *et al*., 2009; Kamimura *et al*., 2017). Furthermore, vanillin was released during WS-BSG fermentation by *L. plantarum* strains, which could originate from the degradation of its glycosylated form. Whether no overexpression was found for the *pbg8* gene, we hypothesize that glycosylated phenolic compounds present in WS-BSG were metabolized by other *pbg* genes associated to generic β-glucoside PTS (Filannino *et al*., 2018).

A release of syringic acid and vanillin was also found for *Leuc. pseudomesenteroides* DSM 20193 during WS-BSG fermentation. Conversely, DSM 20193 does not harbour the above-mentioned dehydrogenases. Hence, we hypothesize that the acidification might have solubilized lignin subunits, leading to an increase in syringic acid and vanillin Filannino *et al*., 2018b).

Together, the results presented in this study demonstrated that the ability of *L. plantarum* and *Leuc. pseudomesenteroides* to ferment lignocellulose-derived substrates is related to the capacity of bacteria to rapidly adapt and use the available nutrients for growth. The model system applied here and the reconstruction of the metabolic network through phenomics will help to elucidate the processes that underlie specific behaviour during WS-BSG fermentation processes. The chemical composition of WS-BSG substrate caused the phenotypic switching of the bacteria metabolism towards pathways involving the metabolism of saccharides derivatives of hemicelluloses and celluloses, thus modifying the overall BSG rheology and nutritional features. Among *L. plantarum* strains, PU1 showed the greatest highest metabolic flexibility during WS-BSG fermentation while putative deglycosylation and degradation of lignin building blocks was proposed. The *in vivo* phenomes will allow greater understanding of how lactic acid bacteria transform BSG into food ingredients, releasing flavour and bioactive compounds, and overall modifying BSG functional properties. Our study might be also useful for further development of prebiotic applications, by using WS-BSG as natural functional components, even in combination with potential probiotic lactic acid bacteria to design synbiotic products.

Experimental procedures

Preparation of media

The company Peroni Srl (Bari, Italy) kindly supplied brewers' spent grains (BSGs) at 4°C which were aliquoted and stored at −20°C until further processing. BSGs derived from the production of a lager beer brewed with barley malt (70%) and maize (*Zea mays*) (30%) and do not contain spent yeast. BSGs were grinned with a laboratory mill Ika-Werke M20 (GMBH, and Co. KG, Staufen, Germany). WS-BSG medium was chosen as model system representative of water-soluble fraction of the BSG ecosystem. Briefly, WS-BSG medium was obtained from BSG through a multi-step sequential process. One hundred grams of BSG was homogenized with 40% of distilled water, incubated for 18 h at 25°C under stirring conditions (100 rpm), centrifuged (10 000 × *g* for 20 min at 4°C), sterilized by filtration on 0.22 μm membrane filters (Millipore, USA) and stored at −20°C before use. Rich De Man, Rogosa and Sharpe (MRS) medium (Oxoid, United Kingdom) was used as the control for optimal lactic acid bacteria growth. The main chemical composition of the WS-BSG medium is shown in Table S1 in the supplemental material.

Microorganisms and growth condition

Lactiplantibacillus plantarum PU1, H46 and WCFS1 obtained from the Culture Collection of the Department of Soil, Plant and Food Science of the University of Bari Aldo Moro (Bari, Italy) and *Leuconostoc pseudomesenteroides* DSM 20193 obtained from the Leibniz Institute DSMZ (Braunschweig, Germany) were used in this study. These strains were previously characterized for pro-technology (e.g. acidifying and growth capacity) and functional features (e.g. *L. plantarum* PU1 and H46 for the ability to increase the antioxidant activity during WS-BSG fermentation and *Leuc. pseudomesenteroides* DSM 20193 to synthetize dextran in different food substrates) (Verni *et al*., 2020; Koirala *et al*., 2021). The aptitude of

L. plantarum strains and *Leuc. pseudomesenteroides* DSM 20193 to ferment WS-BSG was also preliminarily verified (Verni *et al*., 2020; Koirala *et al*., 2021). Cultures were maintained as stocks in 15% (vol/vol) glycerol at −80°C. Culture inocula were prepared by harvesting cells during the late exponential growth phase (ca. 8 h) in MRS broth. Cells were washed twice in 50 mM sterile potassium phosphate buffer (pH 7.0). The initial cell number of *L. plantarum* strains and *Leuc. pseudomesenteroides* DSM 20193 used to inoculate WS-BSG medium was ca. 7.0 Log CFU·ml^{-1}. All strains were cultivated in MRS as a control condition. Incubation was performed at 30°C for 24 h (Verni *et al*., 2020). Biologically independent triplicates were performed for each condition. Kinetics of growth were determined by routinely plate count procedure at different time points. Data were modelled according to the logistic equation available in *grofit* R package (Kahm *et al*., 2010). A is the maximum absorbance reached by the culture at the stationary phase of growth (expressed as log CFU·ml^{-1}), μ_{max} is the maximum growth rate (expressed as log CFU·ml^{-1} h^{-1}) and λ is the length of the latency phase (expressed in h). The pH was measured by a Crison pH-meter (model 507; Crison, Barcelona, Spain).

Determination of organic acids and sugars

Every four hours throughout the growth kinetics in WS-BSG and MRS, one millilitre of cell suspensions was collected and centrifuged (10 000 rpm for 5 min), and then the supernatant was filtered through a Millex-HA 0.22-μm-pore-size filter (Milli-pore, MO, USA) and stored at −20°C until further use. Analytical grade organic acids (citric acid, malic acid, acetic acid and lactic acid) and sugar (glucose, fructose and sucrose) standards were purchased from Sigma-Aldrich (Steinheim, Germany). Organic acids of each time point were determined through high-performance liquid chromatography (HPLC) analysis (Dionex UltiMate 3000, Thermo Scientific, MA, USA), equipped with an isocratic pump (P1000), a multiple autosampler (AS3000) fitted with a 20-μl loop and a UV detector operating at 210 nm. The analyses were performed isocratically at 0.8 ml min^{-1} and 65°C with a 300 × 7.8 mm i.d. cation exchange column (Aminex HPX-87H, Biorad, Hercules, USA) equipped with a cation H+ microguard cartridge (Bio-Rad Laboratories, Hercules, CA). Mobile phase was 0.013 N H_2SO_4 prepared by diluting reagent grade sulfuric acid with distilled water, filtering through a 0.45-μm membrane filter (Sartorius, AG, Germany) and degassing under vacuum (Zeppa *et al*., 2001; Tlais *et al*., 2020). Concentration of sucrose, glucose and fructose was determined through HPLC equipped with a Spherisorb column (Waters, Millford, USA) and a IDEX RefractoMax520 refractive index detector. Elution was at 32°C, with a flow rate of 1 ml min^{-1}, using acetonitrile 80% as mobile phase (Rizzello *et al*., 2010).

Phenotypic microarray analysis

Differences in phenotypes under various growth conditions were monitored using OmniLog Phenotype MicroArray (PM) Technology (Biolog). PM plates (Biolog) containing 190 carbon sources (PM1 and PM2) were used. Phenotypic microarray analyses were performed with two biological replicates for each growth condition in accordance with the manufacturer's instructions. Cells were collected when the late exponential (LE) growth phase was reached after ca. 16 h on WS-BSG medium and ca. 8 h on MRS. Then, cells were washed in 50 mM sterile potassium phosphate buffer (pH 7.0), diluted (to achieve 65% transmittance) in inoculating fluid (Biolog) to inoculate the PM plates. One hundred μl of cell suspension was added per each well. Plates were incubated for 48 h at 33°C in an OmniLog automated incubator/reader (Biolog). During incubation, reduction in tetrazolium dye by respiring cells was measured in each well every 15 min by the OmniLog system. Generated longitudinal data were analysed using the *Micro4Food PM* pipeline (Acin-Albiac *et al*., 2020). Briefly, blank subtraction was performed, and metabolic profiles were categorized as active and non-active. Metabolic signals were normalized per replicate and array (Vehkala *et al*., 2015). After removal of common non-active profiles, metabolic parameters were computed using a free splines method and confidence intervals (CI) were determined though bootstrapping (Kahm *et al*., 2010). Since metabolic profiles of *L. plantarum* strains were similar, Bayesian approach was used to investigate the effect of culture media and strains genotype on the metabolism dynamics for the analysed substrates (Vehkala *et al*., 2015). After grouping and normalization procedures, logistic and linear models were fit to the active and non-active profiles respectively. Normalization among replicates was performed using a modification Levenberg–Marquardt algorithm. Aggregated effects of the conditions on the metabolic profiles over time (averaged estimates) and the changes in dynamics between individual time points (time point-wise estimates) were considered. Posterior distribution of each effect parameter was simulated in WinBUGS (Lunn *et al*., 2000) interfaced via R software (R Core Team, 2020). The average values of the simulated Markovian chains were considered as the estimates for strain and culture media effects for each time point analysed (Vehkala *et al*., 2015). The overall capacity of each *L. plantarum* strain to perform a phenotypic switch was evaluated as the proportion of positive, negative and not significant effect during all time points evaluated.

HPLC-MS/MS analysis of phenolic compounds

Cell suspensions of *L. plantarum* PU1 and WCFS1 and *Leuc. pseudomesenteroides* DSM 20193 respectively grown on WS-BSG medium at 30°C for 24 h were harvested (after different times: 0, 2, 4, 6, 8, 13, 16, 20 and 24 h), centrifuged at 10.000 rpm for 5 min, and the supernatant was filtered and stored at −20°C until further use. LC-MS/MS analysis of phenolic acids and other polyphenols of supernatants was carried out using a UHPLC Dionex 3000 (Thermo Fisher Scientific, Germany), coupled to an TSQ Quantum™ Access MAX Triple Quadrupole Mass Spectrometer (Thermo Fisher Scientific) equipped with an electrospray source. Separation of the phenolic compounds was achieved on a Waters Acquity HSS T3 column 1.8 μm, 100 mm × 2.1 mm (Milford, MA, USA), kept at 40°C. Mobile phase A was water containing 0.1% formic acid; mobile phase B was acetonitrile containing 0.1% formic acid. Flow was 0.4 ml min^{-1}, and the gradient profile was 0 min, 2% B; from 0 to 3 min, linear gradient to 20% B; from 3 to 4.3 min, isocratic 20% B; from 4.3 to 9 min, linear gradient to 45% B; from 9 to 11 min, linear gradient to 100% B; from 11 to 13 min, wash at 100% B; from 13.01 to 15 min, back to the initial conditions of 5% B. The injection volume of both the standard solutions and the samples was 3 μl. After each injection, the needle was rinsed with 600 μl of weak wash solution (water/methanol, 90:10) and 200 μl of strong wash solution (methanol/water, 90:10). Samples were kept at 4°C during the analysis (Vrhovsek *et al*., 2012). Selected chemical standards were used to perform calibration curves, and data were expressed as mg l^{-1} of WS-BSG medium. The target phenols were detected under multiple reaction monitoring (MRM) mode, and the compounds were identified based on their reference standard, retention time and qualifier and quantifier ion. The chromatographic system and the data acquisition were managed by Xcalibur software version 4.1 (Thermo Fisher Scientific, Germany).

Phospho-beta-glucosidase sequence analysis

Leuc. pseudomesenteroides DSM 20193 genome (NCBI: txid33968) was reannotated using RAST server (Aziz *et al*., 2008). Sequences for each gene encoding for phospho-beta-glucosidase enzymes for *L. plantarum* and *Leuc. pseudomesenteroides* were downloaded from KEGG (https://www.genome.jp/kegg/) and retrieved from the reannotated genome respectively. Sequences were aligned using MAFFT with L-INS-I option to increase the accuracy (Katoh and Standley, 2013). Tree topology construction was computed through PhylML (Guindon *et al*., 2010). The amino acid substitution model that maximizes the likelihood score and best fits the data was selected according to Akaike Information Criterion (AIC). The reliability of generated topology was evaluated through bootstrapping using 100 samplings.

Primer design for selected genes

Sequences for all gene targets for *L. plantarum* and *Leuc. pseudomesenteroides* were downloaded from KEGG (https://www.genome.jp/kegg/) and retrieved from the reannotated genome respectively. Single-nucleotide polymorphisms (SNP) were masked to avoid designing primers over those regions and were used as an input in Primer-BLAST. Primer specificity was checked against the corresponding representative genomes. Primer length was set from 18 to 24 pb, amplicon length 80-250 pb, primer Tm from 54 to 59°C for *L. plantarum* PU1 and WCFS1 and from 62 to 65°C for *Leuc. pseudomesenteroides* DSM 20193 with maximum 2°C difference. % GC content target was set at 50% ranging from 40 to 60%. GC clamp was set at 1 in order to force the inclusion of a G or a C at primer 3' end, which enhances the binding at extension site (Bustin and Huggett, 2017). To increase the accuracy on the design, thermodynamic alignments were used in Primer-Blast, whose results were checked for putative secondary nucleotide structures at 59 and 65°C in a concentration of 0.05 and 0.015 M of Na^{+} and Mg^{++}. Hairpins and primer dimer structures were evaluated through DINAmelt two State folding and melting (Markham and Zuker, 2008). Primer sets were discarded if the free energy (ΔG) was below −2.5 kcal mol^{-1} (Table S2). Overall, primer quality and linguistic complexity were checked using FastPCR software (Kalendar *et al*., 2017). Primer pair was accepted if both parameters were above 75% as recommended for qPCR applications (Kalendar *et al*., 2017).

RNA isolation and transcript analysis by quantitative Real-Time PCR (RT-PCR)

Total RNAs were obtained from 1 ml of *L. plantarum* PU1, WCFS1 and *Leuc. pseudomesenteroides* DSM 20193 cells respectively grown in WS-BSG medium at 30°C until the LE phase of growth was reached (after ca. 16 h). Since all strains showed a diauxic kinetic for the organic acid production in WS-BSG medium, total RNAs was also obtained from cultures after ca. 8 h of phase of growth. Total RNAs were also obtained from cells grown in MRS at 30°C until the LE phase of growth was reached (after ca. 8 h).

Samples (ca. 8 log CFU ml^{-1}) were centrifuged at 9000 × *g* for 10 min at 4°C, and RNA isolation was performed with Stool Total RNA purification kit as recommended by the manufacturer (Norgen, Thorold, Canada)

with some modifications. Cells were lysed using 200 μl of lysozyme 15 mg ml^{-1} and 20 μl of Proteinase K (Qiagen, Hilden, Germany) for 45 min at 25°C under constant shaking (2000 rpm). Seven hundred μl of lysis buffer was added to the mixture and shaken vigorously. Five hundred μl of propanol was used to precipitate the nucleic acids. Lysate was loaded into the column following manufacturer's instructions. Total RNA was treated with RNase-free Turbo™ DNase (Ambion, TX, USA). Quality and quantity control of RNA were obtained on agarose-gel electrophoresis and. by NanoDrop ND-1000 spectrophotometer (Thermo Fisher, MA, USA) respectively.

Total RNA was transcribed to cDNA using random hexamers priming and the Tetro cDNA synthesis kit according to the manufacturer's instructions (Bioline, London, UK). To assess the specificity of this newly designed primer pairs, qPCR reactions were carried out using gDNA from *L. plantarum* PU1, WCFS1 and *Leuc. pseudomesenteroides* DSM 20193. PCR amplification products were further loaded on agarose 4% gel to check whether they corresponded exactly to amplicon size (Fig. S1). All reactions were set up in a QuantStudio 5 (Applied Biosystems, Germany) equipped with a 96 well reaction block. The reaction mixture (20 μl) contained 10 μl of TB Green™ Premix Ex Taq™ II (Tli RNaseH Plus) qPCR master mix (Takara, Japan), 1 μl cDNA sample and appropriate primer concentration (Table S2. Assays were carried out in triplicate. PCR required an initial denaturation at 95°C for 30 s, followed by a 40-cycle amplification consisting of denaturation at 95°C for 5 s, annealing for 34 and 30 s for *Leuc. pseudomesenteroides* DSM 20193 and *L. plantarum* strains respectively, and the extension was for 34 and 40 s respectively (Table S2). Fluorescence signals were normalized according to ROX reference dye levels. After the last cycle of each amplification, a melt curve analysis, with a temperature range from 60 to 95°C ramping at 1°C/5 s, was performed to determine the product specificity. Gene expression data were normalized to levels of the 16S rRNA housekeeping gene and analysed using a comparative cycle threshold method ($\Delta\Delta C_T$). Levels of expression of genes were compared using the relative quantification method (Derveaux *et al.*, 2010; Applied Biosystems, 2018). Real-time data are shown as the relative change compared to *L. plantarum* PU1 and *Leuc. pseudomesenteroides* DSM 20193 grown in MRS. Error bars show the standard deviations (SD) of the $\Delta\Delta C_T$ value.

Statistical analysis

R software version 3.6.1 was used to analyse the data (R Core Team, 2020). Data of growth kinetics and relative fold change were subjected to one-way or two-way analysis of variance (ANOVA), and pairwise comparison of treatment means was achieved by Tukey's procedure at a P value of < 0.05, using Tukey–Kramer test through *HSD.test* function available in *agricolae* R package (De Mendiburu, 2020). The AUC of phenotype analysis was subjected to clustering analysis using the Manhattan distance matrix and ward.D2 method available in default *dist* and *hclust* functions available in R (R Core Team, 2020).

Acknowledgements

This work was supported by the Open Access Publishing Fund of the Free University of Bozen-Bolzano.

This transnational project is part of the ERA-Net SUSFOOD2 with funding provided by national/regional sources [FORMAS, Sweden; Ministry of Agriculture and Forestry of Finland; MIUR, Ministero Italiano dell'Università e della Ricerca] and co-funding by the European Union's Horizon 2020 research and innovation programme.

Conflict of interest

The authors have no conflict of interest to declare.

References

Acin-Albiac, M., Filannino, P., Gobbetti, M., and Di Cagno, R. (2020) Microbial high throughput phenomics: the potential of an irreplaceable omics. *Comput Struct Biotechnol J* **18:** 2290–2299.

Applied Biosystems (2018) *Real-Time PCR handbook*. https://www.thermofisher.com/content/dam/LifeTech/global/Forms/PDF/real-time-pcr-handbook.pdf.

Aziz, R.K., Bartels, D., Best, A.A., DeJongh, M., Disz, T., Edwards, R.A., *et al.* (2008) The RAST Server: rapid annotations using subsystems technology. *BMC Genom* **15:** 1–15.

Bustin, S., and Huggett, J. (2017) qPCR primer design revisited. *Biomol Detect Quantif* **14:** 19–28.

Côté, G.L., and Skory, C.D. (2012) Cloning, expression, and characterization of an insoluble glucan-producing glucansucrase from Leuconostoc mesenteroides NRRL B-1118. *Appl Microbiol Biotechnol* **93:** 2387–2394.

Delgado, S., Flórez, A.B., Guadamuro, L., and Mayo, B. (2017) Genetic and biochemical characterization of an oligo-α-1,6-glucosidase from Lactobacillus plantarum. *Int J Food Micobiol* **246:** 32–39.

De Mendiburu, F. (2020) Package ' agricolae.'

Derveaux, S., Vandesompele, J., and Hellemans, J. (2010) How to do successful gene expression analysis using real-time PCR. *Methods* **50:** 227–230.

Desroche, N., Beltramo, C., and Guzzo, J. (2005) Determination of an internal control to apply reverse transcription quantitative PCR to study stress response in the lactic acid bacterium Oenococcus oeni. *J Microbiol Methods* **60:** 325–333.

Duar, R.M., Lin, X.B., Zheng, J., Martino, M.E., Grenier, T., Pérez-Muñoz, M.E., *et al*. (2017) Lifestyles in transition: evolution and natural history of the genus Lactobacillus. *FEMS Microbiol Rev* **41:** S27–S48.

Esteban-Torres, M., Reverón, I., Plaza-Vinuesa, L., de las Rivas, B., Muñoz, R., and López de Felipe, F. (2017) Transcriptional reprogramming at genome-scale of Lactobacillus plantarum WCFS1 in response to olive oil challenge. *Front Microbiol* **8:** 1–10.

Filannino, P., Cardinali, G., Rizzello, C.G., Buchin, S., De Angelis, M., Gobbetti, M., and Di Cagno, R. (2014) Metabolic responses of Lactobacillus plantarum strains during fermentation and storage of vegetable and fruit juices. *J Appl Environ Microbiol* **80:** 2206–2215.

Filannino, P., De Angelis, M., Di Cagno, R., Gozzi, G., Riciputi, Y., and Gobbetti, M. (2018) How *Lactobacillus plantarum* shapes its transcriptome in response to contrasting habitats. *Environ Microbiol* **20:** 3700–3716.

Filannino, P., Di Cagno, R., Crecchio, C., De Virgilio, C., De Angelis, M., and Gobbetti, M. (2016) Transcriptional reprogramming and phenotypic switching associated with the adaptation of *Lactobacillus plantarum* C2 to plant niches. *Scien Rep* **6:** 1–16.

Filannino, P., Di Cagno, R., and Gobbetti, M. (2018) Metabolic and functional paths of lactic acid bacteria in plant foods: get out of the labyrinth. *Curr Opin Biotechnol* **49:** 64–72.

Gänzle, M.G. (2012) Enzymatic synthesis of galacto-oligosaccharides and other lactose derivatives (hetero-oligosaccharides) from lactose. *Int J Dairy Technol* **22:** 116–122.

Gänzle, M.G., and Follador, R. (2012) Metabolism of oligosaccharides and starch in lactobacilli: a review. *Front Microbiol* **3:** 1–15.

Gobbetti, M., Lavermicocca, P., Minervini, F., De Angelis, M., and Corsetti, A. (2000) Arabinose fermentation by *Lactobacillus plantarum* in sourdough with added pentosans and α-L-arabinofuranosidase: a tool to increase the production of acetic acid. *J Appl Microbiol* **88:** 317–324.

Guindon, S., Dufayard, J.-F., Lefort, V., Anisimova, M., Hordijk, W., and Gascuel, O. (2010) New algorithms and mehtods to estimate maximum-likelihood phylogenies: asessing the performance of PhyML 2.0. *Syst Biol* **59:** 307–321.

Guyot, J.P., and Morlon-Guyot, J. (2001) Effect of different cultivation conditions on *Lactobacillus manihotivorans* OND32T, an amylolytic lactobacillus isolated from sour starch cassava fermentation. *Int J Food Microbiol* **67:** 217–225.

Inglin, R.C., Meile, L., and Stevens, M.J.A. (2018) Clustering of Pan- and Core-genome of Lactobacillus provides novel evolutionary insights for differentiation. *BMC Genom* **19:** 1–15.

Kahm, M., Hasenbrink, G., and Ludwig, J. (2010) grofit : Fitting biological growth curves with R. *J Stat Softw* **33:** 1.

Kalendar, R., Khassenov, B., Ramankulov, Y., Samuilova, O., and Ivanov, K.I. (2017) FastPCR: an in silico tool for fast primer and probe design and advanced sequence analysis. *Genomics* **109:** 312–319.

Kamimura, N., Goto, T., Takahashi, K., Kasai, D., Otsuka, Y., Nakamura, M., *et al*. (2017) A bacterial aromatic aldehyde dehydrogenase critical for the efficient catabolism of syringaldehyde. *Sci Rep* **7:** 1–12.

Katoh, K., and Standley, D.M. (2013) MAFFT multiple sequence alignment software version 7: improvements in performance and usability. *Mol Biol Evol* **30:** 772–780.

Koirala, P., Maina, N.H., Nihtilä, H., Katina, K., and Coda, R. (2021) Brewers' spent grain as substrate for dextran biosynthesis by Leuconostoc pseudomesenteroides DSM20193 and Weissella confusa A16. *Microb Cell Fact* **20:** 23.

Ktenioudaki, A., Chaurin, V., Reis, S.F., and Gallagher, E. (2012) Brewer's spent grain as a functional ingredient for breadsticks. *Int J Food Microbiol* **47:** 1765–1771.

Lao, E.J., Dimoso, N., Raymond, J., and Mbega, E.R. (2020) The prebiotic potential of brewers' spent grain on livestock's health: a review. *Trop Anim Health Prod* **52:** 461–472.

Lunn, D.J., Thomas, A., Best, N., and Spiegelhalter, D. (2000) WinBUGS – A Bayesian Modelling Framework: concepts, structure, and extensibility. *Comput Stat* **10:** 325–337.

Lynch, K.M., Steffen, E.J., and Arendt, E.K. (2016) Brewers' spent grain: a review with an emphasis on food and health. *J Inst Brew* **122:** 553–568.

Markham, N.R., and Zuker, M. (2008) UNAFold: software for nucleic acid folding and hybridization. *Methods Mol Biol* **453:** 3–31.

Martino, M.E., Bayjanov, J.R., Caffrey, B.E., Wels, M., Joncour, P., Hughes, S., *et al*. (2016) Nomadic lifestyle of Lactobacillus plantarum revealed by comparative genomics of 54 strains isolated from different habitats. *Environ Microbiol* **18:** 4974–4989.

Mazzoli, R., Bosco, F., Mizrahi, I., Bayer, E.A., and Pessione, E. (2014) Towards lactic acid bacteria-based biorefineries. *Biotechnol Adv* **32:** 1216–1236.

Mendis, M., and Simsek, S. (2014) Arabinoxylans and human health. *Food Hydrocoll* **42:** 239–243.

Mota, L.J., Tavares, P., and Sá-Noguelra, I. (1999) Mode of action of AraR, the key regulator of L-arabinose metabolism in *Bacillus subtilis*. *Mol Microbiol* **33:** 476–489.

Mussatto, S.I. (2014) Brewer's spent grain: a valuable feedstock for industrial applications. *J Sci Food Agric* **94:** 1264–1275.

Olvera, C., Centeno-Leija, S., and López-Munguía, A. (2007) Structural and functional features of fructansucrases present in Leuconostoc mesenteroides ATCC 8293. *Antonie van Leeuwenhoek J Microbiol* **92:** 11–20.

Özcan, E., Selvi, S.S., Nikerel, E., Teusink, B., Toksoy Öner, E., and Çakır, T. (2019) A genome-scale metabolic network of the aroma bacterium Leuconostoc mesenteroides subsp. cremoris. *Appl Microbiol Biotechnol* **103:** 3153–3165.

R Core Team (2020) *R: A Language and Environment for Statistical Computing*.

Redon, E., Loubiere, P., and Cocaign-Bousquet, M. (2005) Transcriptome analysis of the progressive adaptation of *Lactococcus lactis* to carbon starvation. *J Bacteriol* **187:** 3589–3592.

Rencoret, J., Prinsen, P., Gutiérrez, A., Martınez, Á.T., and del Rıo, J.C. (2015) Isolation and structural characterization of the milled wood lignin, dioxane lignin, and

cellulolytic lignin preparations from brewer?s spent grain. *J Agric Food Chem* **63:** 603–613.
Rizzello, C.G., Nionelli, L., Coda, R., De Angelis, M., and Gobbetti, M. (2010) Effect of sourdough fermentation on stabilisation, and chemical and nutritional characteristics of wheat germ. *Food Chem* **119:** 1079–1089.
Robertson, J.A., I'Anson, K.J.A., Treimo, J., Faulds, C.B., Brocklehurst, T.F., Eijsink, V.G.H., and Waldron, K.W. (2010) Profiling brewers' spent grain for composition and microbial ecology at the site of production. *LWT - Food Sci Technol* **43:** 890–896.
Rodríguez, H., Curiel, J.A., Landete, J.M., de las Rivas, B., de Felipe, F.L., Gómez-Cordovés, C., *et al*. (2009) Food phenolics and lactic acid bacteria. *Int J Food Microbiol* **132:** 79–90.
Shalini, R., and Gupta, D.K. (2010) Utilization of pomace from apple processing industries: a review. *J Food Sci Technol* **47:** 365–371.
Siezen, R.J., and van Hylckama Vlieg, J.E.T. (2011) Genomic diversity and versatility of *Lactobacillus plantarum*, a natural metabolic engineer. *Microb Cell Fact* **10:** S3.
Tarraran, L., and Mazzoli, R. (2018) Alternative strategies for lignocellulose fermentation through lactic acid bacteria: the state of the art and perspectives. *FEMS Microbiol Lett* **365:** 126.
Teusink, B., Wiersma, A., Molenaar, D., Francke, C., de Vos, W.M., Siezen, R.J., and Smid, E.J. (2006) Analysis of growth of *Lactobacillus plantarum* WCFS1 on a complex medium using a Genome-scale Metabolic Model. *J Bio. Chem* **281:** 40041–40048.
Thompson, J., Jakubovics, N., Abraham, B., Hess, S., and Pikis, A. (2008) The sim operon facilitates the transport and metabolism of sucrose isomers in Lactobacillus casei ATCC 334. *J Bacteriol* **190:** 3362–3373.
Thongaram, T., Hoeflinger, J.L., Chow, J., and Miller, M.J. (2017) Prebiotic Galactooligosaccharide metabolism by probiotic Lactobacilli and Bifidobacteria. *J Agric Food Chem* **65:** 4184–4192.
Tlais, A.Z.A., Da Ros, A., Pasquale, F., Vicentini, O., Gobbetti, M., and Di Cagno, R. (2020) Biotechnological recycling of apple by-products: a reservoir model to produce a dietary supplement fortified with biogenic phenolic compounds. *Food Chem* **336:** 127616.
Vehkala, M., Shubin, M., Connor, T.R., Thomson, N.R., and Corander, J. (2015) Novel R pipeline for analyzing biolog phenotypic microarray data. *PLoS One* **10:** 1–14.
Verni, M., Pontonio, E., Krona, A., Jacob, S., Pinto, D., Rinaldi, F., *et al*. (2020) Bioprocessing of Brewers' spent grain enhances its antioxidant activity: characterization of phenolic compounds and bioactive peptides. *Front Microbiol* **11:** 1–15.
Vrhovsek, U., Masuero, D., Gasperotti, M., Franceschi, P., Caputi, L., Viola, R., and Mattivi, F. (2012) A versatile targeted metabolomics method for the rapid quantification of multiple classes of phenolics in fruits and beverages. *J Agric Food Chem* **60:** 8831–8840.
Watson, D., O'Connell Motherway, M., Schoterman, M.H.C., van Neerven, R.J.J., Nauta, A., and Van Sinderen, D. (2013) Selective carbohydrate utilization by lactobacilli and bifidobacteria. *J Appl Microbiol* **114:** 1132–1146.
Zeppa, G., Conterno, L., and Gerbi, V. (2001) Determination of organic acids, sugars, diacetyl, and acetoin in cheese by high-performance liquid chromatography. *J Agric Food Chem* **49:** 2722–2726.
Zhao, X., and Gänzle, M.G. (2018) Genetic and phenotypic analysis of carbohydrate metabolism and transport in *Lactobacillus reuteri*. *Int J Food Microbiol* **272:** 12–21.

Supporting information

Additional supporting information may be found online in the Supporting Information section at the end of the article.

Dataset S1. Metabolic parameters determined using phenotype microarrays (Omnilog, Biolog) of Leuconostoc pseudomesenteroides DSM 20193 and Lactobacillus plantarum WCFS1, PU1 and H46 cultured in the soluble fraction of water-soluble brewers' spent grain extract (WS-BSG) and in MRS compromising 190 carbon sources. Sources not listed where common non-active profiles for all conditions and strains.

Figure S1. Agarose gel electrophoresis of the amplified genomic DNA for Leuconostoc pseudomesenteroides DSM 20193 (PS) and Lactobacillus plantarum WCFS1 (LP) employing the newly designed primers (Table S2), as detailed in Experimental procedures – Primer design for selected genes section. M; TrackIt Ultra Low Range DNA ladder (Invitrogen, USA).

Figure S2. Logistic median metabolic curves of active profiles changing activity of Lactobacillus plantarum PU1, H46, WCFS1 cultured in water-soluble brewers' spent grain extract (WS-BSG) (continuous line) and MRS (dashed line) used for the variance analysis model.

Figure S3. Estimate effects and 95% Bayesian credibility intervals over time computed as the mean values of Markov chains produced by the variance analysis model. Effects evaluated are culture media [water-soluble brewers' spent grains (WS-BSG) and MRS], strain (Lactobacillus plantarum PU1, H46, WCFS1) and their interactions. MRS – L. plantarum PU1 represents the reference condition.

Figure S4. Phenolic profile evolution of water-soluble brewers' spent grain extract (WS-BSG) fermented with Lactobacillus plantarum PU1 and WCFS1, and Leuconostoc pseudomesenteroides DSM 20193 for 24 h at 30°C.

Figure S5. Phylogenetic trees based on the amino acid sequences of re-annotated genome of Leuconostoc pseudomesenteroides DSM 20193 and phospho-beta-glucosidases from the genomes of five Lactiplantibacillus plantarum strains used as references. Sequences were annotated according to their operon organization with β-glucosides or cellobiose transporter systems (PTS). Purple circles represent the bootstrap value for a clade within a minimum value of 7 up to 100.

Table S1. Main chemical composition of brewers' spent grains (BSG) medium.

Table S2. Primers designed in this study. F corresponds to Forward and R to Reverse primer.

